Magnetic nanoparticle design for medical diagnosis and therapy

Stéphane Mornet, Sébastien Vasseur, Fabien Grasset, Etienne Duguet

Magnetic nanoparticle design for medical diagnosis and therapy

Stéphane Mornet, Sébastien Vasseur, Fabien Grasset and Etienne Duguet*

Institut de Chimie de la Matière Condensée de Bordeaux, CNRS/université Bordeaux-1, 87 avenue du Dr Albert Schweitzer, F-33608 Pessac Cedex, France.
E-mail: duguet@icmcb.u-bordeaux1.fr

Magnetic nanoparticles have attracted attention because of their current and potential usefulness as contrast agents for magnetic resonance imaging (MRI) or colloidal mediators for cancer magnetic hyperthermia. This review examines these *in vivo* applications through an understanding of the involved problems and the current and future possibilities for resolving them. A special emphasis is made on magnetic nanoparticle requirements from a physical viewpoint (*e.g.* relaxivity for MRI and specific absorption rate for hyperthermia), the factors affecting their biodistribution (*e.g.* size, surface hydrophobic/hydrophilic balance, *etc.*) and the solutions envisaged for enhancing their half-life in the blood compartment and targeting tumour cells.

Introduction

The history of magnetism in medicine is old and is punctuated with amazing anecdotes about the pioneering work of physicians and physicists.[1] The first medical uses of magnetite powder for internal applications were reported by the Egyptian physician and philosopher Avicenna in the 10th century A.D. He recommended the use of one magnetite grain as an antidote for the accidental swallowing of rust. Taken with milk, the magnetite was believed to render the poisonous iron inert by attracting it and speeding up its excretion through the intestine. An earlier use of a magnetic force was where iron particles embedded in the eye were removed. More recently, miniaturization of electromagnets, development of

---

Dr Stéphane Mornet received his Ph.D. in the physico-chemistry of condensed matter from the University of Science and Technology of Bordeaux under the supervision of Professor Etienne Duguet, in 2002. Then, he moved to the European Institute of Chemistry and Biology in the Molecular Imaging and NanoBiotechnology Laboratory of Bordeaux for a post-doctoral position. On the interface of chemistry and biology, his research focuses on the synthesis of magnetic and luminescent nanoparticles, their surface functionalisation and conjugation with biological matter for imaging and therapy purposes.

Sébastien Vasseur was born in 1978. He received a B.Sc. degree in chemistry from the Ecole Normale Supérieure of Lyon. He is currently carrying out a Ph.D. in nanotechnology and applications in biology under the supervision of Professor Etienne Duguet at the University of Science and Technology of Bordeaux.

Dr Fabien Grasset received his Ph.D. in solid state chemistry from the University of Science and Technology of Bordeaux in 1998. After a post-doctoral stay at the Institute of Condensed Matter Chemistry of Bordeaux in collaboration with Professor Etienne Duguet, he undertook a post-doctoral fellowship at the National Institute for Materials Science in Japan from 1999 to 2001. He is currently associate professor at the University of Rennes and his area of research interest at the Laboratory of Glasses and Ceramics focuses on oxides and oxynitrides colloids.

Professor Etienne Duguet was born in 1965. He received an engineer diploma from the National School of Chemistry and Physics of Bordeaux in 1988 and a Ph.D. degree in polymer chemistry from the University of Science and Technology of Bordeaux in 1992. He is currently full professor and his research at the Institute of Condensed Matter Chemistry of Bordeaux focuses on the synthesis of hybrid organic–inorganic materials based on inorganic particles derivatized through molecular surface modification, polymer encapsulation, dissymetrization and/or functionalisation for optical or medical applications.

superconducting electromagnets and introduction of strong permanent magnets (Sm–Co and Nd–Fe–B) have stimulated the medical use of magnets in fields as diverse as dentistry, cardiology, neurosurgery, oncology, radiology, *etc*. For instance, miniaturized strong magnets can fit into the tip of catheters, permitting their magnetic guidance from outside the body. For stereotactic neurosurgery, very strong superconducting magnets were designed for delivering small magnetic Nd–Fe–B capsules within the brain with an accuracy of 2 mm. External magnets can also be employed to stop intravenously (*i.v.*) injected magnetic microspheres at or in a target organ, *e.g.* a tumour. Thus, accumulation of microspheres filled with chemo- or radio-therapeutic drugs in the target area leads to an efficient drug delivery, lowers drug systemic toxicity and can sometimes mechanically block the vessels and capillaries (chemoembolization).

A further medical use of magnets extends to modern diagnostic methods such as magnetic resonance imaging (MRI) taking advantage of the magnetic properties of hydrogen present in the body tissues (in water, membrane lipids, proteins, *etc.*). So, MRI is routinely used for three-dimensional non-invasive scans of the human body and is currently the most important diagnostic method available. Early in the development of MRI, it was thought that contrast agents would not be necessary, but it has become increasingly clear that, in many clinical situations, contrast agents can greatly improve the diagnostic value of MRI. Indeed, one of the most effective techniques for altering the relaxivity of water is to introduce a high spin paramagnetic metal complex, *e.g. i.v.*-injected Gd^{3+}-chelates are routinely used as MR contrast agents. More recently, aqueous dispersions of magnetite nanoparticles embedded in dextran corona have been designed for a similar task.[2]

Since it is now accepted that magnetic fields are not especially contraindicated for humans, except for patients whose body contains magnetizable material (medical devices with batteries or computer chips, vascular or intracranial metallic material), the therapeutic potential of magnetism has arisen when hyperthermia, *i.e.* heat treating, has been recognized as a promising form of cancer therapy, particularly in synergy with chemo- and/or radio-therapy. As the healing power of heat has been established for a very long time and used to cure a variety of different diseases,[3] a novel hyperthermia route for homogeneously treating deep or scattered tumours would consist of concentrating magnetic nanoparticles around and inside the tumorous tissue and making them heat through energy absorption from an external alternating magnetic field (magnetic hyperthermia).

Whatever the applications in both MRI and hyperthermia, the use of magnetic nanoparticles in the blood compartment depends on specific requirements with respect to their plasma half-life and their final biodistribution. The problem of the non-natural stealthiness of the nanoparticles towards the immune system and the possibilities for resolving it have been widely studied in the field of drug delivery from polymeric nanoparticles and liposomes.[4] Indeed, retention of drugs in circulation is a key step in the design of drug delivery devices. Even the most active compound *in vitro* is useless if it does not reside *in vivo* in the blood compartment long enough to reach its target, while managing to avoid to some extent premature metabolism, immunological reactions, toxicity, rapid excretion and captation by undesired tissues.[5] Today, much information is now available about the immune system mechanisms, the factors affecting the biodistribution of polymeric nanoparticles, such as their size and shape, hydrophobic/hydrophilic balance of their surface, surface charge, *etc.*, and the solutions envisaged for targeting specific organs or tumour cells.[5]

The aim of this review is to describe the potential *in vivo* applications of magnetic nanoparticles. This description requires the understanding of the problems involved from the viewpoint of their overall requirements, for their synthesis and bulk and surface properties. Physical background for such nanoparticles was recently reviewed.[6] One of the main intentions of the present contribution is to impart information about both the state of the art as well as the need for further progress and clinical development. Only typical examples will be reported and discussed and a special emphasis will be made on cancer diagnosis and therapy.

What happens to nanoparticles after *i.v.* injection in the blood compartment

Intravenous administration is the most useful method to reach target organs and tissues, because all vital cells receive supplies by means of the blood circulation. The fundamental question of the nanoparticles' fate in the blood compartment has been widely discussed by physicians and scientists involved in the design and the development of devices for controlled drug delivery. These colloidal drug carriers are essentially liposomes and polymeric particles.[5]

Liposomes are based on water-insoluble polar lipids (*e.g.* phospholipids), which arrange themselves in an excess of water into concentric and closed membranes. Their diameter ranges from 50 nm for the smallest unilamellar vesicles (SUVs) to several micrometers for the multilamellar type (MLVs). The classical preparation procedure consists of dissolving appropriate amounts of phospholipids in an organic solvent, evaporating it and subsequently disrupting the dry lipid layer with excess water or buffer, leading to the spontaneous formation of multilamellar liposomes of heterogeneous size. They can become SUVs with prolonged sonication time. Drugs may be entrapped either in the inner aqueous phase or in the lipid bilayers, depending on their hydrophilicity/hydrophobicity ratio.

Biodegradable polymeric particles are defined as spheres when made of a solid polymer framework or as capsules when consisting of a central liquid cavity surrounded by a polymer wall. The first generation, made of starch, albumin, poly(lactic acid), *etc.*, was in the micrometer range, so they cannot pass through capillaries and must be implanted as close as possible to their target. They are essentially used for chemoembolization: drugs localize in the nearby tissue surrounding the capillaries where microparticles accumulate by upstream intra-arterial injection. The second generation consists in nanoparticles which are able to pass through capillaries and therefore are suitable for systemic use. They are capable of not only protecting the active molecule and releasing it at the target site, but also carrying it there. Various methods and polymers can be used for particle preparation:[5] polyalkylcyanoacrylate (PACA) nanospheres of around 150 nm in diameter are synthesized through an oil/water emulsion polymerisation (anionic mechanism), polyisobutylcyanoacrylate nanocapsules (200–300 nm) by interfacial polymerisation, polylactide nanospheres by precipitation in heterogeneous medium, *etc*. The drug entrapping step is generally performed simultaneously to the polymerisation one. The release of the entrapped drugs, peptides or proteins is controlled by the diffusion rate across the polymer framework or the erosion rate of the biodegradable matrix. Compared to liposomes, polymeric nanoparticles exhibit the advantage of the possibility to modulate the drug release profile and are more stable after contact with biological fluids.[7] For more information about the synthesis and the potential medical applications of polymeric nanoparticles, recent and complete review papers may be consulted for an overview[8–10] or for specific purposes such as the targeted delivery of antibiotics,[11] brain delivery of drugs[12,13] or cancer therapy.[14]

The mononuclear phagocyte system and the passive targeting route

The mononuclear phagocyte system (MPS), alternatively known as the reticuloendothelial system, is defined as the cell family comprising bone marrow progenitors, blood monocytes and tissue macrophages (such as Kupffer cells in the liver).[15] These macrophages are widely distributed and strategically placed in many tissues of the body to recognize and clear senescent cells, invading micro-organisms or particles.[9] The first step of the clearance mechanism is the opsonization process. Opsonins are circulating plasma proteins (various subclasses of immunoglobulins, complement proteins, fibronectin, *etc.*), which adsorb themselves spontaneously onto the surface of any invading entity. They are capable of interacting with the specialized plasma membrane receptors on monocytes and macrophages, thus promoting particle recognition by these cells. On exposure to blood, particles of different surface characteristics, size and morphology attract different arrays of opsonins, the content and conformation of which may account for the different pattern in the rate and site of particle clearance from the blood compartment.[16] The second step consists of the endocytosis/phagocytosis of the particles by the circulating monocytes or the fixed macrophages, leading to their elimination from circulation and their simultaneous concentration in organs with high phagocytic activity. Therefore after *i.v.* administration, colloidal drug carriers are cleared up within minutes from the bloodstream and their typical final biodistribution is of 80–90% in the liver, 5–8% in the spleen and 1–2% in the bone marrow.[5]

Consequently, the remarkable organization of the immune system is not compatible with long circulation times of any invading nanoparticle and MPS-mediated clearance is a major factor in determining their biodistribution.[17] Nevertheless, it has provided an opportunity for the efficient delivery of therapeutic agents to these phagocytic cells and therefore to the related organs. Such an MPS-mediated targeting is called passive targeting. For instance, PACA nanospheres loaded with doxorubicin may be used for the treatment of hepatic metastases.[18] Moreover, the passive targeting of antibiotics to phagocytic cells of the MPS improves the treatment of intracellular infections compared with treatment using free antibiotics.[11]

Long-circulating nanoparticles as the first requirement for active targeting

If monocytes and macrophages in, or in contact with, blood are not the desired target, a strategy of active targeting has to be developed and its first requirement consists of minimizing or delaying the nanoparticle uptake by the MPS.[9]

A classical approach is the prior *i.v.* injection of large doses of placebo nanoparticles in an effort to impair the phagocytic capacity of macrophages. Another one consists of the transient destruction of liver and spleen macrophages by prior administration of gadolinium chloride particles or liposomes with entrapped clodronate, which induces apoptosis (programmed cell death, *i.e.* cell suicide). If promising results were obtained *in vitro* in various models of autoimmune diseases and gene transfer protocols involving adenoviruses, this strategy has little justification in clinical practice as it suppresses the essential defence system of the body.

Therefore the most satisfactory strategy consists of using macrophage-evading nanoparticles, with a plasma half-life as long as possible in order to increase the probability of attaining the desired target. The design of such stealth nanoparticles may be inspired by Nature's principles.[9] For example, healthy erythrocytes (red blood cells) evade the macrophages and fulfil their function of transporting oxygen with a life span of 110–120 days. A multitude of physico-chemical and physiological factors are believed to ensure this long circulation time. In particular, their surface protection by a barrier of hydrophilic oligosaccharide groups is thought to prevent the opsonin adsorption and therefore to avoid the macrophage recognition.

Among the physico-chemical factors which are known for having an effect on the opsonization process, the size, the surface charge density and the hydrophilicity/hydrophobicity balance have been widely studied, either in liposome or polymeric nanoparticle systems.[9] The main conclusion is that the smaller, the more neutral and the more hydrophilic the carrier surface, the longer its plasma half-life. Concerning the size effect, this indicates that surface curvature changes may affect the extent and/or the type of opsonin adsorption.

It is generally assumed that surface features are more important than those of the core, because the surface is in direct contact with the blood and organs.[19] For hydrophobic carriers, many studies have concerned the development of core–corona structures where the corona is made of hydrophilic macromolecules for creating polymer brushes, acting as a steric surface barrier and reducing opsonin adsorption. Among the natural or artificial macromolecules, linear dextrans and derivatives are widely used. They are produced by bacterial fermentation of sucrose, followed by hydrolysis and fractionation to give macromolecule sets with different average molecular weights (Fig. 1). Linear dextrans have frequently been used as plasma expanders in medicine: drugs conjugated to dextran remain in the blood circulation for extended periods of time which are proportional to the average molecular weight of the macromolecules. The clearance rate of dextran-coated liposomes is dependent on the density of dextran molecules on the liposome surface.[9] Other biological macromolecules have been investigated, *e.g.* poly(sialic acid), heparin and heparin-like polysaccharides complement regulatory proteins, *etc.*, but because of their high cost and/or the possible immunological consequences associated with bacterial-made macromolecules, efforts have been directed to the design of synthetic hydrophilic macromolecules.

Among these synthetic macromolecules, the adsorption of block-copolymers such as poloxamers and poloxamines (Fig. 1) has been widely studied.[20] Poloxamers consist of a central hydrophobic poly(propylene oxide) (PPO) block that is flanked on both sides by two hydrophilic chains of poly(ethylene oxide) (PEO). Poloxamines are tetrafunctional block-copolymers with four PPO/PEO blocks joined together by a central

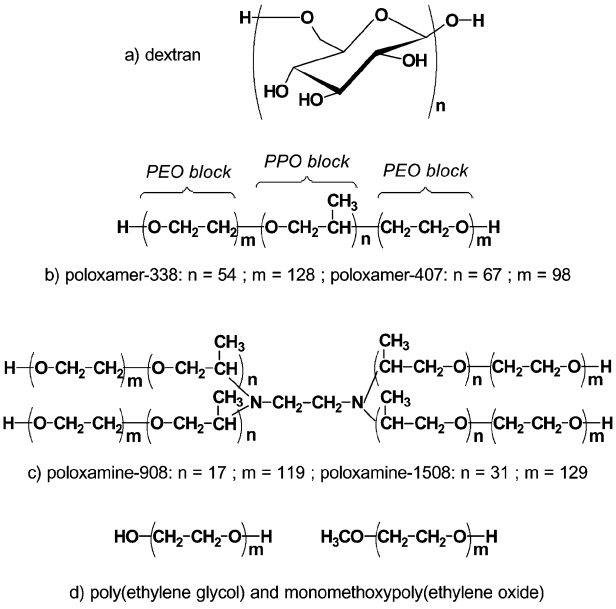

Fig. 1 Typical macromolecules used as hydrophilic coating for MPS-evading nanoparticles.

ethylenediamine bridge. Such copolymers adsorb onto the surface of any hydrophobic surface *via* their hydrophobic PPO center-block. This mode of adsorption leaves the hydrophilic PEO side-arms in a mobile state so that they extend outward from the particle surface. The strength of polymer adsorption and the resultant polymer conformation is dependent on the proportion and the size of both PPO and PEO blocks as well as the physico-chemical properties and the curvature of the nanoparticle surface.[20,21] The particle stealthiness is believed to be a function of the thickness and the density of the PEO layers. For example, reported half-lives of poloxamine-908-coated nanospheres in mice and rats may reach 1–2 days.[20] Interestingly, it has been shown that *i.v.*-injected uncoated 60 nm (hydrophobic) polystyrene nanoparticles were converted into long-circulating entities in rats that received a bolus *i.v.* dose of poloxamer 1–3 h earlier.[22] Therefore it would seem that nanoparticles acquire a coating of copolymer and/or copolymer–protein complexes in the blood; the surface modification prior to *i.v.* injection would not be really necessary.

Nevertheless, in particular to avoid the possible depletion of copolymers in the blood compartment, great efforts have dealt with the covalent anchorage of PEO macromolecules onto the carrier surface. Such a route is well-known in galenical pharmacology where drugs (small molecules, but also peptides, proteins, antibodies and oligonucleoides) are conjugated to PEO macromolecules in order to improve their circulation lifetime, bioavailability and decrease their immunogenicity, renal clearance rate and dosing frequency.[5] This process is so widely used that it is called 'PEGylation', derived from PEG for poly(ethylene glycol). In actual fact, PEG is only the α,ω-dihydroxyl derivative of PEO. PEO is a flexible polyether, hydrophilic (but also soluble in some organic media), not biodegradable, but easily excreted from living organisms. Its functional end-groups are available for derivatization leading to numerous routes for covalent attachment onto preformed functional surfaces or anchoring during the synthesis of polymeric particles.[23] PEO has been shown to be the most effective polymer for suppressing protein adsorption, the optimal molecular weight varying between 2000 and 5000 g mol^{-1}.[7,9]

Lastly, regardless of the active targeting strategy, long-circulating carriers present also a great interest as circulating drug reservoirs (for drugs or therapeutic agents with short elimination half-lives) or for blood-pool imaging in nuclear medicine.[9] Moreover, long-circulating particles' escape from the circulation is normally restricted to sites where the capillaries have opened fenestrations, such as in the sinus endothelium of the liver, or when the integrity of the endothelial barrier is perturbed by inflammatory processes (*e.g.* rheumatoid arthritis, infarction, infections) or by some types of tumours.[9] Therefore the idea of exploiting such vascular abnormalities for extravasating and accumulating nanoparticles in these inflammatory sites or tumours is also particularly attractive. Such a strategy is also considered as a passive targeting one, but independently of the MPS mediation (Fig. 2).

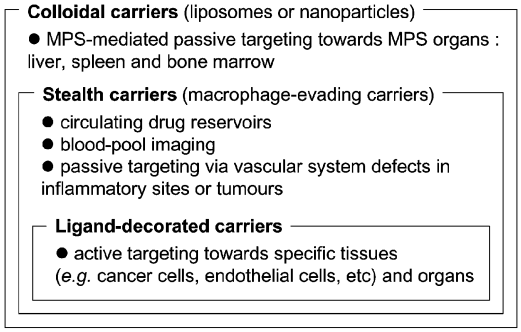

Fig. 2 Typical potential applications of drug carriers as a function of their degree of sophistication.

Ligand conjugation as the second requirement for active targeting

For increasing the probability of redirecting long-circulating particles to the desired target, their surface has to be labelled with ligands that specifically bind to surface epitopes or receptors on the target sites (molecular recognition processes such as antibody–antigene interactions). These ligands have to be not macrophage-recognizable and coupled to the surface of stealth carriers. Such a strategy should open the possibility of targeting specific cell types or subsets of cells within the vasculature and even elements of vascular emboli and thrombi.[9] In the case of cancer therapy, active targeting could allow the selective destruction of cancer cells, even if they have escaped the tumour mass and disseminated as metastatic cells. Initial efforts have focused on long-circulating liposomes through the attachment of ligands to PEG-grafted vesicles.[9] On the contrary, few studies have dealt with ligand-mediated targeting of polymeric nanoparticles.[24–27]

These ligands include oligosaccharides, oligopeptides, folic acid, antibodies and their fragments. The antibody coupling has at least two drawbacks: the overall dimensions of the antibodies (*ca.* 20 nm), which cause particles to diffuse poorly through biological barriers; and their immunogenicity, *i.e.* the property of being able to evoke an immune response within an organism. For this reason the coupling of small non-immunogenic ligands to polymeric carriers has been also investigated. Therefore for tumour targeting, folic acid (vitamin B essential for cell division processes) was grafted to PEGylated PACA nanoparticles in order to take advantage of the frequent overexpression of folate receptors onto the surface of human cancer cells.[27] Interestingly, nanoparticles conjugated with folic acid appeared to interact more efficiently with folate receptors than free folic acid. This amazing result was interpreted as the consequence of the multivalent (and hence stronger) interaction of conjugated nanoparticles with the folate receptors which are often arranged as clusters. Moreover, confocal microscopy demonstrated that conjugated nanoparticles, compared to non-conjugated nanoparticles, are localized in the cell cytoplasm of folate receptor-bearing cells, as a consequence of folate receptor-mediated endocytosis. It was checked that cells devoid of folate receptor did not internalise conjugated nanoparticles. So not only do nanoparticles conjugated with folic acid selectively target cancer cells, but they could also improve the internalisation of the encapsulated drugs into the targeted cancer cells.

Magnetic nanoparticles as contrast agents for MRI

Magnetic resonance imaging (MRI) applications have steadily widened over the past decade. Currently, it is the preferred cross-sectional imaging modality in most diseases of the brain, spine and musculoskeletal system.

From MRI physical principles to paramagnetic contrast agents (T_1-agents)

MRI is based on NMR signal of protons from water in tissues, membrane lipids, proteins, *etc.*, through the combined effect of a strong static magnetic field B_0 up to 2 T in current clinical apparatus and a transverse radiofrequency-field (rf-field) (5–100 MHz).[6] After the rf-sequence, the net magnetization vector (NMV) is once again influenced by B_0 and tries to re-align with it along the longitudinal axis as protons attempt to return to a state of equilibrium: this phenomenon is called relaxation. This relaxation can be divided into two different, independent processes: (i) longitudinal relaxation, which is the return of longitudinal magnetization in alignment with B_0 and is termed T_1-recovery; and (ii) transverse relaxation, which is the vanishing of transverse magnetization and is termed

T_2-decay. As the hydrogen atoms release the previously absorbed energy to the surrounding tissue (lattice) in their attempt to re-align with B_0, T_1 recovery is also referred to as 'spin–lattice' relaxation. As a time constant, T_1 is the time it takes for 63% of the longitudinal magnetization to recover in the tissue. On the contrary, T_2 decay is not a process of dissipation or absorption of energy into tissue. During the rf-pulse, hydrogen nuclei are spinning in phase with each other. After the rf-pulse, the magnetic fields of all the nuclei interact with each other; energy is exchanged between those nuclei. The nuclei lose their phase coherence and spin in a random fashion. Because T_2 decay is the result of the exchange of energy between spinning protons, it is referred to as 'spin–spin' relaxation. Therefore T_2 is the time it takes for the transverse magnetization to decrease to 37% of its initial value. Owing to their different T_1 and T_2 relaxation, tissues may be differentiated.

In order to correlate the signal to its spatial origin, at least one of the two fields (*i.e.* B_0 or the rf-field) has to vary over space. Relaxation data are collected by a computer which applies a two-dimensional Fourier transform to give the amplitudes of NMR signals and permits reconstruction of the 3-D images. Thanks to sequence parameters, such as the repetition time TR (elapsed time between successive rf excitation pulses) and the delay time TE (time interval between the rf-pulse and the measurement of the first signal), the operator obtains the desired type of image contrast. Basically, short TRs increase T_1 effects, whereas long TRs allow tissues to reach complete longitudinal magnetization, reducing T_1 effects. Short TEs minimize T_2 effects of tissues whereas long TEs allow the loss of transverse signal, enhancing T_2 effects. Therefore T_1-weighted imaging is obtained by utilising a short TR and a short TE, allowing full recovery of tissues with a short T_1 (*e.g.* fat) while allowing only partial recovery of tissues with long T_1 (*e.g.* cerebrospinal fluid). On the other hand, for T_2-weighted imaging, long TRs and long TEs are used. Fluids have a very long T_2 and they are frequently associated with pathologies, *e.g.* internal injuries, cancer lesions, *etc.*, so T_2-weigted images are generally preferred for such diagnostics.

MR contrast may be naturally enhanced by the presence *in vivo* of paramagnetic substances. The ability of such compounds to increase the relaxation rates of the surrounding water proton spins is called relaxivity and is defined as $R_1 = 1/T_1$ or $R_2 = 1/T_2$. Therefore, for instance, the presence of haemoglobin is used in functional MRI (fMRI) to map brain functions, *e.g.* taste, smell, reading, listening, *etc.*[28] Indeed, oxyhaemoglobin (the principal haemoglobin in arterial blood) is diamagnetic (low R_1 relaxivity, *i.e.* without effect on proton relaxation), whereas the deoxygenated form, the deoxyhaemoglobin, is paramagnetic (higher relaxivity, *i.e.* relaxation increase of the surrounding protons). This allows determination of the brain areas which are more or less oxygenated and measurement of blood flow variations. But, in many clinical situations, the intrinsic differences in R_1 (or R_2) between tissues is small and it is now admitted that the use of exogenous contrast media for a better delineation of tissues can greatly improve the diagnostic value of MRI. Although these contrast agents may also be administered by inhalation, oral or interstitial routes,[28] only *i.v.* administration will be discussed in this section.

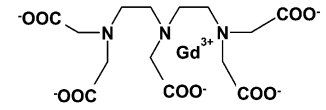

Fig. 3 Gd^{3+}–diethylenetriaminepentaacetate (Gd–DTPA).

The first generation of these contrast agents consists of T_1-agents, *i.e.* high spin paramagnetic ions, usually Gd^{3+} (seven unpaired electrons) in very stable chelate form obtained through complexation by low molecular weight chelating molecules, such as diethylenetriaminepentaacetic acid (DTPA) (Fig. 3, Table 1). The presence of DTPA avoids the inherent toxicity risks of these cations, *e.g.* transient destruction of the MPS macrophages, exchange with endogenous calcium ions, *etc*. Gd-chelates have a non-selective extracellular distribution before their excretion by the kidneys. They have to be administered in concentrations of about 0.1 mmol kg^{-1} of body mass to produce visible effects on the images. Hydrogen atoms of water in proximity to such chelates experience a faster T_1-relaxation. Consequently, differences in agent concentration result in contrast enhancement on T_1-weighted images ('positive' contrast). The process of T_1 shortening requires the direct interaction between protons and the magnetic part of the contrast agent.[28] Gd-chelates are routinely used for distribution into the intravascular and interstitial space to enhance signal of fluid compartments or lesions (renal function, status of the blood–brain barrier, *etc.*).[29] Current developments consist of (i) enhancing the relaxivity of Gd-chelates through the optimisation of the molecular structure, *e.g.* increasing the number of water molecules in the inner sphere of the complex, increasing the water exchange rate, improving the steric hindrance around the Gd^{3+} ion for optimal residence times of the coordinated water in the first coordination sphere, *etc.*,[30] (ii) increasing the plasma half-lives beyond the typical values of 70–100 min, and (iii) increasing the gadolinium concentration at the target. Therefore some contrast agents in development

Table 1 Non-exhaustive list of MR contrast agents which are in use or have been advocated[a]

MR contrast agent	Main use	Molecular weight or PCS size	Relaxivity/(mM s)$^{-1}$	Target	Ref.
Gd–DTPA	T_1-agent	0.6 kDa	$R_1 = 3.7$	• Extracellular	31
Dextran–Gd–DTPA	T_1-agent	75 kDa	$R_1 = 11$	• Blood-pool • Capillary permeability	31
Carboxydextran-coated SPIO SHU-555[b]	T_2-agent	62 nm	$R_1 = 12$; $R_2 = 188$ (0.94 T)	• MPS organs (liver)	45
Dextran-coated SPIO AMI-25[c]	T_2-agent	58 nm	$R_1 = 24$; $R_2 = 107$ (0.47 T)		62
Dextran-coated USPIO MION-46L[d]	T_2-agent	18–24 nm	$R_1 = 16$; $R_2 = 35$ (0.47 T)	• MPS organs	40
Dextran-coated USPIO AMI-227[e]	T_2-agent	17–20 nm	$R_1 = 23$; $R_2 = 53$ (0.47 T)	• Lymph nodes	62
MION-encapsulated liposomes	T_2-agent	170–300 nm	$R_1 = 10$; $R_2 = 130$ (0.47 T)	• MPS organs (liver)	57
PEGylated magnetoliposomes	T_2-agent	40 nm	$R_1 = 3$; $R_2 = 240$ (1.5 T)	• Bone marrow	59
(Protein-coated) magnetoferritin	T_2-agent	12 nm	$R_1 = 8$; $R_2 = 218$ (1.5 T/25 °C)	• Blood-pool	41

[a] Relaxivities were measured at 37 °C and the static magnetic field B_0 expressed in Tesla is noticed in brackets. [b] Ferucarbotran Resovist® from Schering, Germany [c] Endorem® from Guerbet, France or Feridex® from Advanced Magnetics, USA [d] Massachusetts General Hospital, Boston, USA [e] Sinerem® from Guerbet, France or Combidex® from Advanced Magnetics, USA

are designed for increasing simultaneously the concentration of paramagnetic ions and the molecular weight of the contrast agent: Gd–DTPA derivatives conjugated with macromolecules such as dextran[31] (Table 1), liposomes based on Gd–DTPA-conjugated lipids[32] or gadolinium-loaded polymer nanoparticles,[33] *etc*. Other T_1-agents were developed in order to replace Gd-chelates or to be used for complementary purposes: Mn^{2+}-chelates (hepatobiliary distribution for diagnosing liver lesions),[34] iron and manganese metalloporphyrin (for their potential selective retention in tumours),[35] nitroxide radicals,[36] manganese-chelating polyglucoronic acid,[37] PEGylated hydroxyapatite nanoparticles containing manganese ions,[38] *etc*.

Superparamagnetic nanoparticles as MR contrast agents (T_2-agents)

Magnetic nanoparticles, with a size generally between 3 and 10 nm, have also been developed as contrast agents for both standard and functional MR imaging.[39] The superparamagnetic behaviour of these sub-domain magnetic cores is similar to that of paramagnetic substances, in that they lose their magnetization when the magnetic field is removed, but differs by the value of the magnetic moment which is markedly higher. Therefore their relaxivities are much higher than those of Gd-chelates. In most situations, they are used for their significant capacity to produce predominantly T_2-relaxation effects, which result in signal reduction on T_2-weighted images ('negative' contrast). Basically, the phenomenon may be described from the large magnetic field heterogeneity around the nanoparticle through which water molecules diffuse.[28] Diffusion induces dephasing of the proton magnetic moments resulting in T_2 shortening. Such contrast agents are also called susceptibility agents because of their effect on the magnetic field. T_2 shortening is a remote effect, whereas the T_1 shortening process requires a close interaction between the water molecules and T_1-agents. These relaxation mechanisms have been widely described and discussed in the literature.[40–43]

Colloidal T_2-agents are often called (U)SPIO for (Ultrasmall) SuperParamagnetic Iron Oxide (Table 1). They consist of iron oxide cores, whose composition and physico-chemical properties vary continuously from magnetite Fe_3O_4 to maghemite γ-Fe_2O_3. For *i.v.* administration, they are generally synthesized in a one-step process by alkaline coprecipitation of iron(II) and iron(III) precursors in aqueous solutions of hydrophilic macromolecules, *e.g*. dextran,[44] carboxydextran,[45] chitosan,[46] starch,[46] heparin[47] and albumin.[44] These macromolecules serve (i) to limit the magnetic core growth during the synthesis, (ii) to stabilize *via* sterical repulsions the nanoparticle dispersion in water (and later in physiological medium), and (iii) to reduce *in vivo* the opsonization process. These colloidal contrast agents would be more realistically described as several magnetic cores, more or less aggregated, embedded in the hydrophilic macromolecules, which are sometimes cross-linked in a second step for enhancing the mechanical entrapment. The overall hydrodynamic diameter, as measured by photon correlation spectroscopy (PCS), is largely higher than the magnetic core dimensions. Interactions between magnetic cores and macromolecules are weak (essentially Van der Waals and hydrogen interactions)[48] and generally prevent any efficient derivatization of dextran corona without macromolecule depletion.[49] A new generation of T_2-agents, based on maghemite cores covalently bonded to dextran macromolecules, was recently investigated.[50,51] Their preparation consists first in colloidal maghemite synthesis, its surface modification through the grafting of aminoalkylsilane groups and the coupling of partially oxidized dextran *via* formation of an imine bond which may be subsequently stabilized by reductive amination. Such a step-by-step synthesis allows control of the magnetic core size and size distribution and the overall hydrodynamic diameter, thanks to accurate and reproducible experimental conditions, *e.g.* colloidal stability control, dextran molecular weight, *etc*. No fractionation was needed for narrowing the size polydispersity. These stable agents may be derivatized for surface labelling, *e.g.* ligand coupling, PEGylation, *etc.*, and thus they are called VUSPIOs for Versatile USPIOs.[51]

(U)SPIO pharmacokinetics, toxicity and biodistribution properties were studied and allowed to define the potential uses of these contrast agents.[2,52–55] The lethal dose LD_{50} of a dextran–iron oxide complex was found to be 2000–6000 $mg_{Fe}\ kg^{-1}$ of body mass, whereas it is 300–600 $mg_{Fe}\ kg^{-1}$ for pristine iron oxide.[55] The nanoparticles are metabolised in lysosomes and the soluble iron becomes part of the normal iron pool (*e.g.* ferritin, hemosiderin, transferritin, haemoglobin).[28,29] It may be noticed that the iron load resulting from administration of the clinical dose (*ca.* 1 $mg_{Fe}\ kg^{-1}$ of body mass) is low compared with the total store in the human body (about 3500 mg).

It may be noticed that magnetoliposomes could also be used as MR contrast agents (Table 1).[56,57] This type of vesicle consists of nanometer-sized iron oxide particles wrapped in a phospholipid bilayer. Such magnetoliposomes could have structural and biokinetic advantages compared with (U)SPIOs thanks to their ability to permit encapsulation of therapeutic drugs or genes, thus providing a combined diagnostic and therapeutic drug delivery system. Several methods have been described for the preparation of magnetoliposomes: dialysis of SUVs in the presence of magnetite nanoparticles,[58] or lauric acid-stabilized magnetite cores,[59] or extrusion of a mixture of USPIOs with phospholipid–cholesterol large unilamellar vesicles (LUVs).[60] For long-circulating magnetoliposomes, PEGylated phospholipid complexes have to be bound in the bilayer structure. PEGylated magnetoliposomes were found to have good properties as a bone marrow-seeking MR contrast agent,[59] while LUVs containing encapsulated dextran–magnetite particles were used to label human peripheral blood mononuclear cells.[60]

Lastly, an alternative to chemical coprecipitation for preparing magnetic cores as MR contrast agents is biomineralisation.[41] In particular, the iron-storage protein ferritin was used to create organic–inorganic nanocomposites of iron oxides, called magnetoferritin.[61] The protein is first depleted of its native weakly paramagnetic ferrihydrite core, followed by the addition of ferrous iron at high pH and temperature under strictly anaerobic conditions, resulting in the formation of a strongly superparamagnetic core (*ca.* 7 nm in diameter).

Size-dependent distribution in tissues (passive targeting)

Two different classes of iron oxides are currently clinically approved or in phase-III trials, *i.e.* in expanded controlled and uncontrolled clinical trials intended to gather additional information to evaluate the overall benefit–risk relationship of the agent and provide an adequate basis for physician labelling (Table 1). SPIO agents exhibit a high R_2/R_1 relaxivity ratio and, because of their overall size (over 40 nm in diameter), they are efficiently accumulated in MPS organs (*ca.* 80% of the injected dose in liver and 5–10% in the spleen with a plasma half-life lower than 10 min.). Therefore SPIOs decrease the liver and spleen signal within several minutes after *i.v.* administration.[45,62] Malignant tumours or metastases, which are typically devoid of a substantial number of Kupffer cells, appear as hyperintense (bright) lesions contrasted against the hypointense (black) liver on T_2-weighted sequences. SPIOs are routinely administered by drip infusion over a period of 30 min rather than with bolus injections. In spite of its very small hydrodynamic volume, magnetoferritin showed also a rapid blood clearance.[63,64] Uptake in the liver and spleen was observed with no apparent involvement of ferritin receptors, since pre-administration of apoferritin (to saturate receptors) yielded similar results.

USPIOs, also called MIONs (Monocrystalline Iron Oxide Nanocompounds), exhibit an overall hydrodynamic diameter lower than 40 nm (Table 1). Thanks to their small size and the hydrophilicity of their dextran corona, they act as stealth particles. Their plasma half-life is higher than 2 hours[39] and therefore they remain in the blood long enough to act as a blood-pool agents for MR angiography (MRA). Some particles leak into the interstitium, where they are cleared by the macrophages of the lymphatic system or drained *via* the lymphatic system and subsequently accumulated in the lymph nodes.[65] Therefore they allow diagnosis of hyperplastic and tumorous lymph nodes by MR lymphography.[66,67] A decrease in signal intensity indicates active uptake of particles into macrophages in normally functioning nodes, whereas an increase in signal intensity indicates altered capillary permeability in tumours. In comparison with SPIOs, USPIOs exhibit lower relaxivities but the lower T_1/T_2 ratio leads to a higher contrast on T_2-weighted images. This T_1/T_2 ratio is also much more favourable for MRA or for low-field T_1-weighted MR techniques (B_0 lower than 0.5 T).[68]

Towards active targeting and molecular imaging

The clinician's dream of an agent which would accumulate highly and specifically in malignant tumours, allowing an accurate diagnosis at a stage when the disease would be still treatable, is still far from reality.[29] As in radioisotope imaging, ligand-mediated MR contrast agents were designed in particular for tumour diagnosis. Therefore antibodies or fragments and folic acid were conjugated to Gd-chelates.[28,29] Pioneering work about magnetic nanoparticles dealt with the simple adsorption of antibodies.[69] The preparation maintained both the immunoreactivity of the antibody and the full relaxing capability of the magnetite particles. Two years later, investigation with MION was performed with antibody IgG to target sites of acute inflammation.[70] MION was attached to IgG by means of electrostatic adsorption or covalent binding. After *i.v.* administration of MION–IgG to normal rats, most of the particles localized in the liver, spleen and bone marrow. In an animal model of myositis, MION–IgG caused reduced signal intensity on T_2-weighted images at the site of inflammation. No change in signal intensity existed after an injection of unlabelled MION. Later, more sophisticated conjugation to magnetic cores was reported with different ligands, *e.g.* human polyclonal IgG,[70] L6 antibody,[71] *etc*. Investigations in small animals revealed that it is possible to achieve a high concentration of the magnetic label at the target. However, the required dose of the labelled antibody is still too high to make a commercial development realistic.[29] As already discussed about active targeting in drug delivery, folate-mediation appears also promising for tumour MRI diagnostic work. Initial work consisted in the grafting of folic acid to magnetite particles (10 nm in diameter) previously treated with 3-aminopropyltrimethoxysilane.[72] The nanoparticle internalisation into mouse macrophage and human breast cancer cells was checked and quantified. Nevertheless, these investigations were performed without relevant controls and therefore the efficient mediation of folic acid was not demonstrated. Moreover, the preparation step, which consisted of drying the nanoparticles prior to and after surface modification, led obviously to the nanoparticle aggregation preventing any *in vivo* stealthiness towards MPS. Recent work focused on a similar strategy and was based on VUSPIO agents.[73] A controlled amount of folic acid-conjugated PEG macromolecules was chemically bound to the dextran corona of VUSPIO whose surface was subsequently saturated with grafted PEG in order to reduce the opsonization process. A final overall hydrodynamic diameter of *ca.* 50 nm was found. Cell culture contact was performed with three cell lines previously defined for their expression of the specific folate receptor. Folate-labelled VUSPIOs were internalised only in the folate receptor-bearing cells, and PEGylated but unlabelled VUSPIO were not internalised, whatever the cell lines. Future results of MRI experiments on animals with such VUSPIOs are awaited with interest.

Magnetic nanoparticles as mediators for magnetic hyperthermia

About medical benefits of heat

The notion of 'hyperthermia' (Greek word for 'overheating') in the treatment of a large variety of diseases and dysfunctions is as old as medicine itself. Indeed, heat was mentioned as a potential treatment for breast cancer more than 5000 years ago.[74] Since then, methods used for hyperthermia were cauterisation of surface tumours by application of a hot iron, whole-body immersion in a hot water bath, intentional inoculation of pyrogens (*e.g.* bacteria toxins evoking a febrile response from the patient's immune system), *etc*.

Today, hyperthermia remains a promising form of cancer therapy aside from the well-known methods of surgery, chemotherapy and radiotherapy. Two kinds of heating treatments are currently distinguished: (mild) hyperthermia is performed between 41 and 46 °C to stimulate the immune response for non-specific immunotherapy of cancers, and thermoablation (more than 46 °C, up to 56 °C) leads to tumour destruction by direct cell necrosis, coagulation or carbonisation.[75] Clinical experiments taking advantage of the higher sensitivity of tumour cells to temperature in the range of 42–45 °C than normal tissue cells were reported in the 1970s.[76] It is thought that, in such a temperature range, the function of many structural and enzymatic proteins within cells is modified, which in turn alters cell growth and differentiation and can induce apoptosis.[77]

Heat, by its very nature, can be applied locally with no systemic effects and reduced side effects, compared to traditional treatments (chemotherapy drugs have severe side effects on healthy organs and radiotherapy adversely affects nearby tissues). Unfortunately, the temperature at which tumour cell thermoablation occurs is too close to that of normal cells and therefore (unrealistic) temperature control would be required. To overcome this problem, attempts have been made to use (mild) hyperthermia in combination with other treatment modalities such as chemotherapy or irradiation. The latter approach is based on growing knowledge about microenvironmental conditions within the tumour, in particular the fact that hypoxic (poorly oxygenated) cancerous cells are much more resistant to radiation than euoxic (well oxygenated) cancerous cells, whereas hypoxic cells are more heat-sensitive than euoxic cells.[78] Therefore in order to obtain the greatest efficiency in cancerous cell destruction it seems logical to combine these two modalities of cancer therapy. Clinical results showed that the combination of radiation therapy and hyperthermia conducted to a substantial therapeutic improvement.[79] One possible explanation of this combined effect is that heat induces malfunction of repair processes after radiation-induced DNA damage in cancerous cells.[75] It may be noticed that hyperthermia benefits were also reported for various diseases such as gonoccal infection, syphilitic paralysis, *etc.*, and are expected for HIV infection.[80]

From hot water bath to intracellular magnetic hyperthermia

Current modalities for cancer hyperthermia may be classified according to the nature of the heating source and the heated target, from whole-body to tumoral cell level (Table 2).[77,81,82] Main heating sources fall into three categories: contact with externally heated liquid, contactless applicator (*e.g.* ultrasound, microwave, radiofrequency and infrared devices), and

Table 2 Typical hyperthermia strategies in oncology[77,81,82] (in italics: experimental techniques which are currently undergoing preclinical evaluation)

Hyperthermia strategy		Overheated region			
		Whole-body	Organ	Tumour	Tumour cell
Contact with a hot source		• Hot bath, air, wax, blanket, suits, *etc.*	• Isolated organ perfusion (*e.g.* liver)	• Direct injection of hot water (96 °C)	
Ultrasound applicator				• Scanned focused ultrasound monitored by MRI	
Electro-magnetic hyperthermia	Radiative applicator	• Water-filtrated infrared exposure		• Interstitial laser photocoagulation (direct insertion of laser fibres)	
	Capacitive applicator	• Radio-frequency capacitance hyperthermia through two electrodes coupled at the body surface	• Focalised microwave beam through one single element applicator coupled at the body surface	• Rf-antennas based on unipolar or bipolar interstitial electrodes • Interstitial microwave antennas	
	Inductive applicator (magnetic hyperthermia)			• Magnetic interstitial implants hyperthermia • *Arterial embolization hyperthermia (AEH) or direct injection hyperthermia (DIH) of magnetic particles*	• *Intracellular hyperthermia (IH) through ligand-mediated magnetic particle (i.v. administration)*

inserted heating source (*e.g.* probes, antennas, laser fibres and mediators). Among the most recent hyperthermia devices, those which are based on either focused ultrasounds or electromagnetic radiation are commercially available. Nevertheless, none of these devices is able to accurately deliver high heat energy to deeply situated cancers without destroying the surrounding normal tissues, leading to the parallel development of technologies based on inserted heating sources.

Unlike other inserted heating sources, *e.g.* optical fibres, radiofrequency and microwave antennas, mediators convert the electromagnetic energy into heat when exposed to an external electrical or magnetic field. Macroscopic mediators are inserted within the body by surgical intervention, whereas micro- or nano-scale mediators are injected as particle dispersion. They are heated either by capacitive applicators, *i.e.* designed for favouring the electric component of electromagnetic fields (E-field), or by inductive applicators where the electric component is lowered to the benefit of the magnetic one (H-field).[81] For capacitive hyperthermia, mediators would have to be materials with high electric conductivity (heating *via* eddy currents), and for inductive hyperthermia they have to be magnetizable. Nevertheless, capacitive applicators may lead to uncontrolled heating of the body because of the tissue's intrinsic electrical conductivity and/or to electrical field heterogeneities due to differences in tissue dielectrical permeabilities. Therefore inductive mediators seem currently more useful because tissues do not contain intrinsic magnetic materials which could deliver heat in an AC magnetic field. Nevertheless, it is impossible to avoid wholly tissue intrinsic heating *via* eddy currents, since the E-field component is never equal to zero. Therefore, with respect to the patient's comfort, it was found that the product Hv (where H is the amplitude and v the frequency of the AC magnetic field) should be lower than 4.85×10^8 A m^{-1} s^{-1} for a treatment duration of one hour.[3] Moreover, the frequency has to be superior to 50 kHz for avoiding neuromuscular electrostimulation and lower than 10 MHz for appropriate penetration depth of the rf-field.[83]

Interstitial macroscopic mediators for magnetic hyperthermia are generally ferromagnetic rods or seeds directly inserted into tumour tissues.[82] These thermoseeds are typically of the order of 1 mm in diameter and 1–7 cm in length. Various alloys including Ni–Cu, Fe–Pt and Pd–Co have been used and corrosion is prevented by a protective coating or gold platting. Even if this technique has been demonstrated to work in a wide variety of human tumour types *in vivo*, its main limitations are stressful surgical intervention, difficult accessibility to some tumours, potential thermoseed migration and non-uniform temperature pattern. There is, therefore, a possible thermal underdosage of critical regions. It may be noticed that for a similar purpose thin sticks (0.5 cm in length and 0.6 mm in diameter) made of carboxymethylcellulose and magnetite nanoparticles (10 nm in diameter) have been inserted stereotactically into the brain tumour of rats.[84] The advantage of such thermoseeds is their 'heat dissolution' after AC magnetic field application allowing the magnetic nanoparticles to diffuse through the tumour.

The latest magnetic hyperthermia modalities are based on micro- or nano-scale mediators in the form of an injectable colloidal dispersion of magnetic particles and may be performed according three strategies: arterial embolization hyperthermia (AEH), direct injection hyperthermia (DIH), and intracellular hyperthermia (IH)[82] (Table 3). Their use appears as the most promising cancer hyperthermia therapy in particular because of the better temperature homogeneity.[75] Prior to heating, their distribution in tissues may be determined by MRI, taking advantage of their magnetic properties. Moreover, the intracellular route, which is based on *i.v.*-administered stealth magnetic nanoparticles designed for selective uptake by tumour cells, would be the optimal method permitting to

Table 3 Comparison of the three main techniques of magnetic hyperthermia using magnetic particles as mediators[82]

	Arterial embolization hyperthermia (AEH)	Direct injection hyperthermia (DIH)	Intracellular hyperthermia (IH)
Magnetic particle administration	Through the arterial supply of the tumour	Directly injected in the tumour	Arterial embolization or direct injection or ideally *i.v.* injection
Heat origin	Intravascular (within the blood vessels)	Extracellular	Intracellular
Nanoparticle design	Mono- or multi-domain particles	Mono- or multi-domain particles	Mono- or multi-domain nanoparticles with stealthy corona and ligand for *i.v.* injection
Expected advantages	• A more effective tissue temperature distribution due to the concentration gradient of particles through the tumour and the surrounding tissues, with the highest concentration in the tumour (no sharp drop in temperature at the tumour edge)	• Not dependent on an arterial pathway to the tumour: could be applicable to a wide range of tumour types • No consequent risk from arterial catheterisation	• Probable improvement of the treatment efficacy • Treatment of scattered tumours and metastases • Lower and therefore safer required magnetic field
Probable drawbacks	• Not applicable to tumours without a good arterial supply (*e.g.* micrometastases) and tumours outside the liver • Risk of embolization and subsequent ischemic necrosis of normal tissues	• Restricted to tumours which would be accurately visualized and accessible under radiological guidance • Necessity of repeated injections for large or irregularly shaped tumours • Increased risk of needle track implantation or local tumour spread	

Fig. 4 Hysteresis cycle of a multidomain magnetic material (H is the magnetic field amplitude, M is the magnetization of the material) and domain wall displacements in such a material (squares symbolise multidomain material, with magnetization of each domain; arrows on the cycle indicate the way the cycle is described when increasing or decreasing the field amplitude).

selectively overheat tumour cells even in disseminated metastases in any region of the body.

Magnetic hyperthermia mechanisms and technology

The origin of magnetic heating *via* inductive mediators essentially depends on the size and the magnetic properties of particles.[3]

For multidomain ferro- or ferri-magnetic materials, heating is due to hysteresis losses. Indeed, large particles of such materials contain several sub-domains, each of them having a definite magnetization direction. When exposed to a magnetic field, the domain with magnetization direction along the magnetic field axis grows and the other ones shrink. This phenomenon is called 'domain wall displacements' (Fig. 4). As this phenomenon is not reversible, *i.e.* magnetization curves for increasing and decreasing magnetic field amplitudes do not coincide, the material is said to exhibit a 'hysteresis behaviour' and produces heat under an AC magnetic field.

In single-domain particles (superparamagnetic particles) no heating due to hysteresis losses can occur because there is no domain wall. In this case, an external AC magnetic field supplies energy and assists magnetic moments to rotate in overcoming the energy barrier $E = KV$, where K is the anisotropy constant and V is the volume of the magnetic core [Fig. 5(a)]. This energy is dissipated when the particle moment relaxes to its equilibrium orientation (Néel relaxation). This phenomenon is characterised by the Néel relaxation time t_N,

$$t_N = t_0 \, e^{\frac{KV}{kT}}$$

where $t_0 \approx 10^{-9}$ s, k is the Boltzmann constant and T the temperature.[3,85] The frequency ν_N for maximal heating *via* Néel

Fig. 5 (a) Néel rotation of magnetization in a magnetic particle (the particle does not rotate); (b) Brown rotation of a magnetic particle (the particle rotates as a whole).

relaxation is given by the equation $2\pi v_N t_N = 1$.[86] It corresponds to the frequency of the maximum of $\chi''(v)$, imaginary component of the complex magnetic susceptibility $\chi(v) = \chi'(v) - i\chi''(v)$.

For both types of particles, heating can also be due to the rotational Brownian motion within a carrier liquid, *i.e.* the rotation of the magnetic particle as a whole because of the torque exerted on the magnetic moment by the external AC magnetic field [Fig. 5(b)]. In this case, the energy barrier for reorientation of a particle is determined by rotational friction within the surrounding liquid. This rotation is characterised by the Brown relaxation time t_B

$$t_B = \frac{3\eta V_B}{kT}$$

where η is the viscosity of the surrounding liquid and V_B the hydrodynamic volume of the particle.[3,85] The frequency v_B for maximal heating *via* Brown rotation is given by the equation $2\pi v_B t_B = 1$.[86]

Whatever the origin of heating, delivered heat must be measured in order to compare the efficiency of these mechanisms. The specific absorption rate (SAR), also denoted specific loss power, is defined as the power of heating of a magnetic material per gram. SAR is measured as

$$\mathrm{SAR} = C\frac{\Delta T}{\Delta t}$$

where C is the specific heat capacity of the sample (J g^{-1} K^{-1}) and $\Delta T/\Delta t$ is the initial slope of the temperature *versus* time dependence. When nanoparticles are dispersed in a gel or in a liquid, contribution of specific heat capacities of the surrounding media must be taken into account.[87] It is very difficult to give a general theoretical expression of SAR because of the large number of parameters: size, size distribution, shape and chemical composition of particles, frequency and amplitude of the magnetic field, *etc*. For example, the specific absorption rate due to hysteresis losses (SAR_H) is proportional to the product $A \cdot v$, where A is the area of the hysteresis cycle. Owing to strict assumptions about field amplitude and particle arrangement in this field,[3] equations may be proposed, but these theoretical trends are not always validated by experimental SAR measurements. For instance, the frequency-dependence law of SAR was found to be different according to the frequency range.[85]

Concerning the electromagnetic devices used for magnetic hyperthermia, the technology of an AC magnetic field is still under development. Most magnetic hyperthermia experiments were done with laboratory-made generators in the frequency range of 50 kHz–1 MHz, with magnetic field amplitudes up to a few tens of kA m^{-1}. These parameters depended more on the technical availability of the generators used rather than on theoretical predictions for optimised SAR. Indeed, a frequency scan is technically tricky in this broad frequency range because of frequency-dependent skin effects and resistance of magnetic applicators. Therefore very few extensive data were reported.[85,86] The majority of hyperthermia experiments were performed in an induction coil or in the air-gap of a magnetic inductor, cooled by water or air (Fig. 6).

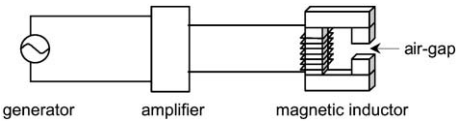

Fig. 6 Typical features of an AC magnetic field air-gap applicator.

At least two full-sized human prototypes have been built by MFH Hyperthermiesystem GmbH, Berlin[88] and Sirtex Medical Ltd, Sydney and will be used shortly for the first clinical trials of hyperthermia.

About optimal physical features of magnetic particles for hyperthermia

For clinical purposes, the value of SAR is crucial because the higher the specific absorption rate, the lower the injected dose to the patient. The results published prior to 1998 were thoroughly reviewed a few years ago[3] and the physical limits of hyperthermia using magnetic nanoparticles were discussed by the same authors.[89] Recent results are also reported in Table 4.[54,89–91] Nevertheless, it may be noticed that no systematic study was reported where each significant parameter (*e.g.* magnetic core size and shape, polymer corona nature and thickness, experimental conditions of synthesis, surrounding liquid, *etc.*) has been independently varied, and a great part of the current knowledge is based on calculations.

Heating of ferromagnetic particles is essentially due to hysteresis losses and Brownian relaxation losses. For the former phenomenon, high magnetic field amplitudes (at least the coercitive field value) are required for using the loop area fully and therefore increasing the SAR_H values. For instance, with magnetic particles of high shape anisotropy (needle-shape particles initially designed for magnetic recording media), hysteresis losses could be higher than all the others if driven to saturation (SAR_H estimation of 2.4 kW g^{-1} for 100 kA m^{-1}).[89] Unfortunately, the hysteresis loop can rarely be fully used because of physiological and technical restrictions on the field amplitude. As a consequence, in clinically tolerable conditions SAR values of large multidomain particles are usually low (Table 4). It was also reported that SAR_H would follow a

Table 4 Specific absorption rates of various magnetic particles

Magnetic nanoparticle			Experimental conditions				
Magnetic compound	Core diameter/nm	Corona	H/kA m^{-1}	*v*/kHz	Dispersion medium	SAR/W g_{Fe}^{-1}	Ref.
Single-domain ferrite	10–12	Dextran	7.2	880	Physiological solution	210 ± 8	54
Single-domain ferrite	6–12	Carboxymethyl dextran	7.2	880	Physiological solution	90 ± 4	54
Multidomain Fe_3O_4	100–150	None	7.2	880	Physiological solution	45 ± 3	54
Multidomain γ-Fe_2O_3	100–150	None	7.2	880	Physiological solution	42 ± 3	54
Single-domain Fe_3O_4	8	None	6.5	300	Water	21[a]	89
Fe_3O_4 (Endorem®)	6	Dextran	6.5	300	Water	<0.1	89
Multi-crystallite needle-shape	50 × 1500	None	14	300	[b]	3	89
Multidomain Fe_3O_4	crushed, *ca.* 350	None	14	300	[b]	75	89
Single-domain γ-Fe_2O_3	[b]	None	8.0	1000	Water	115	90
Single-domain γ-Fe_2O_3	[b]	Dextran (9 kDa)	8.0	1000	Water	170	90
Single-domain γ-Fe_2O_3	[b]	Dextran (>70 kDa)	8.0	1000	Water	400	90
Single-domain γ-Fe_2O_3	3	Dextran	12.5	500	Water	106	91
Single-domain γ-Fe_2O_3	5	Dextran	12.5	500	Water	524	91
Single-domain γ-Fe_2O_3	7	Dextran	12.5	500	Water	626	91

[a] 97 W g_{Fe}^{-1} as calculated for 14 kA m^{-1} assuming square dependence of SAR on the field amplitude. [b] No data.

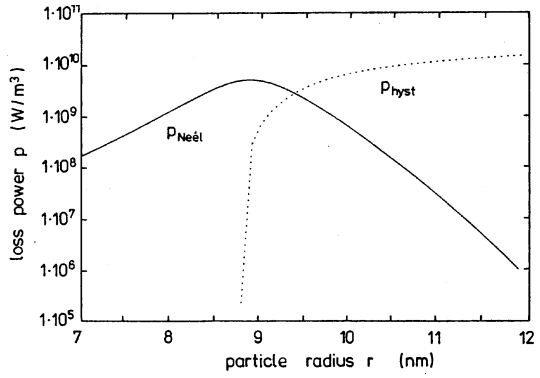

Fig. 7 Dependence of SAR on particle size for magnetite fine powders in rf-field (2 MHz, 6.5 kA m^{-1}): dotted line – hysteresis losses, full line – Néel losses. (Reprinted from ref. 89. © 1998 IEEE.)

non-monotonous dependence on particle size.[89] Hysteresis losses would increase with decreasing particle size due to increasing remanence and coercitivity and then abruptly decrease in the transition region to superparamagnetic behaviour (Fig. 7).

Indeed, when the diameter of the magnetic core is decreased, the transition from ferromagnetic to superparamagnetic behaviour causes changes of the loss mechanism and, accordingly, of the heating effect. As shown on Fig. 7, in the critical core size region where hysteresis losses vanish, Néel relaxation losses increase. One way to experimentally demonstrate that heating is due to Néel and Brown relaxations and not to hysteresis losses is to apply a static magnetic field in the direction perpendicular to the AC magnetic field.[92] Indeed, SAR_B and SAR_N are drastically reduced when the strength of the static field reaches the value of the AC field.

Today particles used for hyperthermia take advantage of Néel relaxation, because, at least for small field amplitudes, superparamagnetic particles give higher SAR than multidomain particles (Table 4). SAR_N optimisation is currently under investigation and, concerning its dependence on magnetic core size, calculations should allow the optimisation of particle diameter with respect to frequency (Fig. 8).[89] Nevertheless, assumptions made for simplifying calculus are strict and experimental results may differ from theory. One of the most crucial parameters is probably the size distribution of magnetic cores. Magnetic fractionation was applied to a common magnetic fluid based on superparamagnetic nanoparticles of iron oxide coated with dextran (one-step synthesis similar to USPIO synthesis) with an initial average core radius of 5 nm.[91] It was confirmed that in this range of size the larger the magnetic cores and the narrower their distribution, the higher the SAR value (Table 4). Therefore the control of the size distribution is as crucial as the average size.

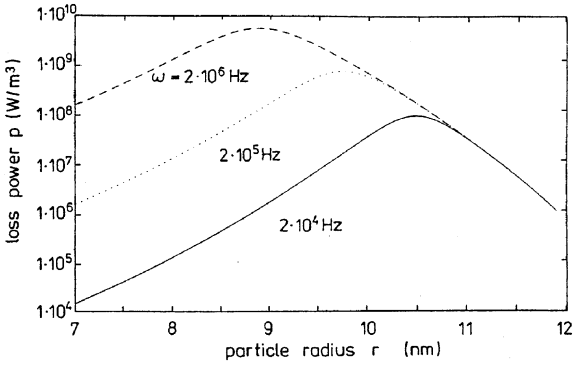

Fig. 8 Simulated grain size dependence of SAR due to Néel relaxation for small ellipsoidal particles of magnetite (rf-field amplitude of 6.5 kA m^{-1}). (Reprinted from ref. 89. © 1998 IEEE.)

Distinguishing contributions of Brown and Néel heating mechanisms seems to be tricky. Theoretically, a critical diameter d_C may be defined as the diameter for which t_N is equal to t_B.[93] For particles of diameter inferior to d_C, Néel relaxation would be predominant. For larger particles, heating would primarily be due to Brownian rotation. When the diameter of the particle is close to d_C, an effective relaxation time must be defined:[94] $t_{eff} = t_N t_B/(t_N + t_B)$. The frequency for maximal heating v_{eff} is then given by the equation $2\pi v_{eff} t_{eff} = 1$. Nevertheless, Brownian relaxation contribution to heating can be experimentally investigated by preventing free rotation of the particle. A comparative study between superparamagnetic (8 nm in diameter) and ferromagnetic (up to several hundred nanometers in diameter) magnetite particles suspended in a commercial gel which melts above 30 °C was reported (Fig. 9).[95] At 410 kHz, with a magnetic field amplitude of 6.5 kA m^{-1}, the heating rate of the gel containing superparamagnetic nanoparticles was about 3.5 °C min^{-1}, with no difference below (Néel relaxation only) and above the melting point (Néel and Brown relaxations). Under the same conditions, the heating rate for ferromagnetic particles was about 1 °C min^{-1} before gel melting (hysteresis losses only) and 15 °C min^{-1} after the melting point (hysteresis losses and Brown relaxation). Brownian losses seem therefore to have a poor effect on SAR for uncoated superparamagnetic particles when compared to uncoated ferromagnetic ones. Indeed, regarding relevant viscosity data, Brownian relaxation of uncoated superparamagnetic particles may be considered as ineffective in biological tissue.[89] But Brownian relaxation depends on the hydrodynamic volume of the particle and not on the volume of the magnetic core, therefore the coating should greatly influence heating *via* a Brownian mechanism. Further investigation about hydrodynamic volume dependence on nanoparticle heating is required and may open new insights for hyperthermia. Indeed, the synthesis conditions and the choice of appropriate polymer corona are of crucial importance.[90] It was shown that for dextran-coated superparamagnetic γ-Fe_2O_3 particles, obtained by addition of a mixture of high molecular weight dextran and ammonia in a solution of iron salts under sonication, the higher the dextran molecular weight, the higher the measured SAR (Table 4). Thanks to experimental conditions (*e.g.* centrifugation and gel-filtration for enriching particles with sizes of 15–30 nm), optimised

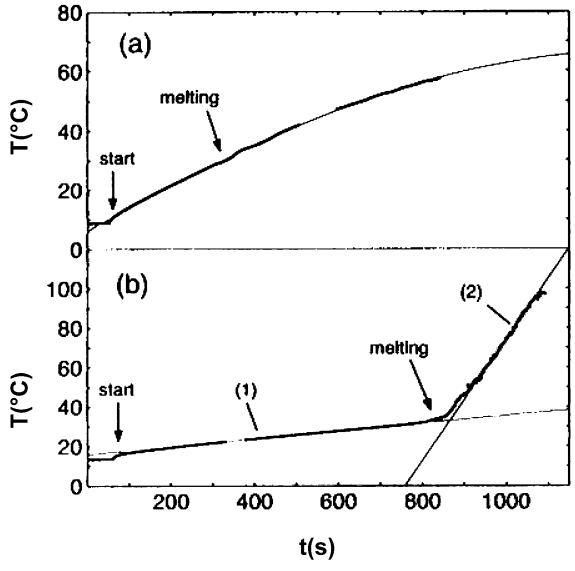

Fig. 9 Temperature increase due to the heating of magnetite particles in rf-field (410 kHz, 6.5 kA m^{-1}) for magnetite ferrofluid (a) and ferromagnetic particles (b), suspended in commercial gel. The starting point of the rf-treatment and melting point of the gel are indicated. (Reprinted from ref. 95, © 1999, with permission from Elsevier.)

colloidal mediators may exhibit 'enhanced' SAR values of 400–500 W g_{Fe}^{-1}.[90]

Choosing high SAR colloidal mediators combined with appropriate technical parameters of the external AC magnetic field, very small amounts of magnetic particles (in the order of a few tenths of milligrams) could be used to perform hyperthermia in biological tissue. The achievement of a well-defined mediator distribution within the tissue is one of the main tasks to be solved on the way to a useful therapy.[89] Therefore today, dispersions of superparamagnetic nanoparticles appear to be all the more promising since they are used as ferrofluids. Such a technology is currently under development as magnetic fluid hyperthermia (MFH).[75] It may be noticed that these ferrofluids are essentially based on oxide nanoparticles and therefore their low electrical conductivities prevent heating *via* eddy current mechanisms.

Nevertheless, ferromagnetic particles remain potentially useful because of their Curie temperature, which could provide one of the more powerful methods for controlling the maximal temperature *in vivo* (see below).

Specific design of magnetic particles for *in vitro* and *in vivo* hyperthermia experiments

Since the pioneering work of Gilchrist *et al.* in 1957,[96] magnetic hyperthermia has been the aim of numerous *in vitro* and *in vivo* investigations.[82] In oncology, three complementary strategies are investigated and some of them are about to be evaluated in clinical trials. They are using magnetic nanocomposite microparticles, surface-modified superparamagnetic nanoparticles (ferrofluids) and ligand-targeted magnetoliposomes, and are developed by Australian, German and Japanese research groups, respectively.

It is now well-established that macroscopic liver tumours derive virtually all their blood supply from the hepatic arterial system, while normal liver tissue receives most of its blood supply from the portal venous system.[97] Taking advantage of such a physiological feature, AEH experiments were performed in rabbits[98] and in pigs[99] demonstrating the higher efficacy of this method in comparison with that of DIH. Indeed, owing to this passive targeting strategy, iron concentration in liver tumours was five times as high as iron concentration in liver normal tissues. First experiments used maghemite submicronic particles (150 nm in diameter) suspended in lipiodol (a sticky mixture of iodine and vegetable oil known for its ability to maintain anticancer drugs in the anarchical blood vessels of tumours).[100] Under inductive applicator conditions of 53 kHz and 30 kA m^{-1}, an intratumoral temperature of 48 °C was reached after 5 min. Because lipiodol proved to be too vaso-occlusive for use in hepatic tissue and led to extensive necrosis,[101] these maghemite particles were encapsulated in polymer matrix beads (SIR-Spheres® from Sirtex Medical Ltd, Sydney, with an average bead diameter of 32 μm) dispersed in a 1% Tween aqueous solution. Such beads appeared to be safe and well-tolerated and neither significant hepatic clearance 28 days after injection nor change in the level of serum iron or ferritin was observed, suggesting that the particles are not digested in ferrous or ferric states. As an extension of the positive results from treating animals, the Sirtex Medical Ltd company is currently investigating the potential use of this technology to treat different forms of human cancer which are not limited to the liver.

Concerning MFH, ferrofluids based on dextran–magnetite nanoparticles have been used since the early 1980s.[102] At this time, it was claimed that some kind of intracellular hyperthermia should occur, if the nanoparticles were taken up by cancer cells. Nevertheless, even if *in vitro* experiments confirmed later that dextran–magnetite nanoparticles may be taken up by carcinoma cells, no additional biological effect of MFH (520 kHz, 7–13 kA m^{-1}) over waterbath heating was observed. However, *in vivo* experiments were performed by intralesional injection into mammary carcinoma transplanted into the right hind leg of mice.[75,103] Before AC magnetic field treatment, magnetic fluid depots in the target region were observed as expected, but after the first MFH session, this distribution had been homogenised. This unexpected phenomenon was described as the 'thermal bystander effect'. Later, dextran–magnetite nanoparticles were classified as unsuitable for an intracellular MFH strategy, because electron microscopy experiments showed that dextran corona may be attacked by enzymes in lysosomes.[104,105] Lastly, magnetite nanoparticles were modified with aminosilane groups (magnetic core diameter 10 nm, hydrodynamic diameter 30 nm) leading to largely positive surface charges in physiological conditions.[106] *In vitro* cellular uptake of aminated-magnetite nanoparticles in glioblastoma cells was 1000 times as large as the uptake of dextran–magnetite nanoparticles, and uptake of both particle types in glioblastoma cells was 500–2000 times as large as in normal cells. Therefore, without a targeting ligand, differential particle endocytosis appeared to be an alternative active targeting strategy. This phenomenon was interpreted as favourable nanoparticle storage by the greedy cancerous cells. Interestingly, it was also observed that tumour cells could be loaded with thousands of nanoparticles and that they would not be able to get rid of them.[75] Daughter cells from a particle-containing parent cell should therefore contain up to 50% of the particle amount of the parent cell. Therefore, the descendants would still be cured by future MFH sessions. This approach for treating glioblastoma led to hopeful reproducible results in animal trials, and very recently the first successful human treatment was carried out on a patient with local residual disease (chondrosarcoma).[107] Moreover, it was claimed that the surface of the nanoparticles used for this therapy may be tuned in order to adapt to certain types of cancer or even to the individual patient tumour (MagForce Applications GmbH, Berlin).

In order to improve the colloidal mediator uptake by cancer cells, monoclonal antibodies IgG were successfully immobilized onto the surface of submicronic magnetite particles (100–200 nm).[108] PEG–magnetite was synthesized through the coprecipitation route in an aqueous solution of α,ω-diamino-PEG. Then, IgG sugar chains were oxidized to give aldehyde groups able to couple with PEG amino groups. The residual antibody activity was about 60%. These particles exhibited a better *in vitro* specificity for cancer cells with an amount of magnetite-labelled antibody adsorbed on the cells, which was about four times that of the control. Under an AC magnetic field (240 kHz, 45.6 kA m^{-1}), the heating rate was about 1.7 °C min^{-1} and the SAR was 31.5 W g^{-1}. Nevertheless, as far as we know, no further *in vitro* or *in vivo* experiments were reported with such IgG-labelled mediators. On the other hand, the same investigators prepared magnetoliposomes by coating phospholipid onto magnetite particles.[109–111] The average size of the magnetoliposomes, which contained aggregates of 10 nm core magnetite particles, was about 80 nm. The IgG antibody and its F(ab′) fragment, specific of the antigen of some gliomal cell lines, were cross-linked to *N*-(6-maleimidocaproyloxy)dipalmitoyl phosphatidylethanolamine in a liposomal membrane. It was found that the F(ab′) fragment is more effective for immobilization (2.4 times higher) than the whole antibody molecule. The fact that the antigenicity of the fragment is lower than that of the whole antibody would be also an advantage in future clinical application. The targetability of the fragment-labelled magnetoliposomes (FMLs) to glioma cells was then investigated. The amount of FML uptake reached 85 pg $cell^{-1}$ in *in vitro* experiments. *In vivo* experiments were performed by the injection into the tumour of glioma-harboring mice (DIH). Approximately 60% of the total injection accumulated in the

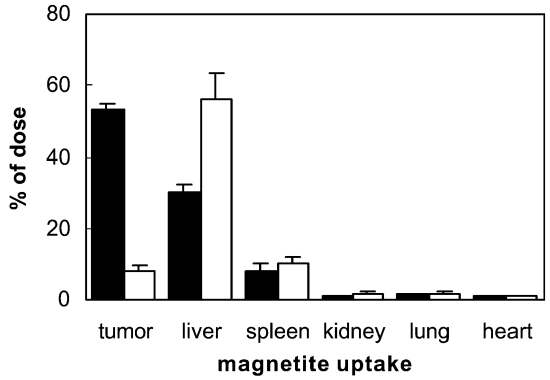

Fig. 10 Intracellular uptake of magnetoliposomes carrying a specific antibody (■) and a non-specific antibody (□) in tumour and various organs. Data and bars are means and standard deviations of five independent experiments. (Redrawn from ref. 110. © 2001 Society of Chemical Engineers of Japan.)

tumour tissue (Fig. 10). The remaining part was removed from the tumour by blood flow and found finally distributed in MPS organs (liver and spleen). Nevertheless, this value was seven times higher than that of magnetoliposomes labelled with a non-tumour-specific antibody. After injection of the FMLs, mice were exposed to an AC magnetic field (118 kHz, 30.6 kA m^{-1}). The temperature of the tumour tissue increased to 43 °C in 30 min and the growth of the tumour was found to be arrested over two weeks.

As far as we know, only one work has yet been reported about *i.v.* administration of colloidal mediators.[102] This very early study consisted of the injection of magnetite nanoparticles (dispersed in a solution of sucrose) into a tail vein of rats containing implanted mammary tumours. As one would expect, tumour cells had indeed taken up particles, but substantial amounts were also present outside the tumour cells, in normal liver tissue and in other tissues such as the spleen and kidney. It is another proof of the necessity of ligand-labelling for active targeting which appears as one of the most promising aspects of hyperthermia mediated by nanoparticles. Nevertheless, it implies a crucial question: is intracellular hyperthermia superior to extracellular hyperthermia? According to a theoretical model, there is no hyperthermic effect at the nanometric scale (particle size) or at the micrometric scale (cell size).[112] Hyperthermia is only possible on a millimetric scale (tumour size), the isolating behaviour of cell membrane being negligable. If any experimental difference is observed between intracellular and extracellular hyperthermia it can only be due to "chemical effects triggered by the presence of the nanoparticles, or mechanical damage caused to the cell by intracellular vibrations and rotations of the nanoparticles".[112]

Towards smart colloidal mediators for self-controlled inductive heating

One of the last crucial steps for clinical application of magnetic hyperthermia remains the temperature control because on the one hand heat conduction and energy adsorption *in vivo* are widely unknown and on the other hand local overheating may damage safe tissue. This problem could be solved by monitoring temperature *via* non-invasive means such as MRI because of the temperature-dependence of proton relaxation times. This strategy is currently being investigated in focused ultrasound hyperthermia where fast MRI has proved to be very efficient for continuous temperature mapping and automatic feedback control of the ultrasound output.[113] It is not obvious that colloidal magnetic mediators do not disturb MR signals and so allow accurate temperature maps.

Another route could exploit the temperature dependence of magnetic properties. Indeed, the Curie temperature (T_C) is the

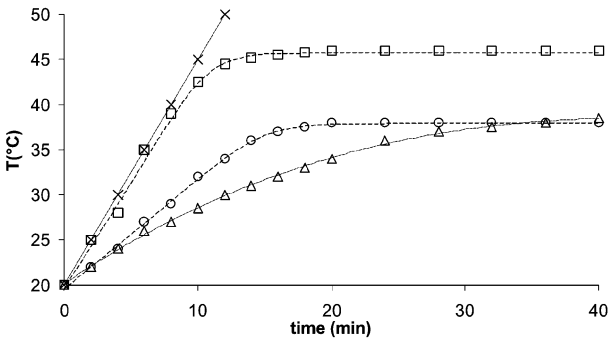

Fig. 11 Time course of the temperature inside the measuring cell during rf-heating (880 kHz, 7.2 kA m^{-1}) using the following mediators: × dextran-coated Fe_3O_4; □ $La_{0.75}Sr_{0.25}MnO_3$; ○ $La_{0.8}Sr_{0.2}MnO_3$; △ $ZnFe_2O_4$. (Redrawn from ref. 114.)

temperature at which ferromagnetic particles lose their magnetic properties, and thus they do not convert electromagnetic energy into heat. The Curie temperature is therefore the maximal temperature reachable by magnetic particles. Choosing an appropriate Curie temperature would be the smartest way to control hyperthermia because in that case particles would be both heaters and fuses. Such a strategy has already been developed for alloy thermoseeds in order to prevent local tissue overheating and reduce the need for invasive thermometry.[82] The design of colloidal mediators was recently reported: $La_{0.8}Sr_{0.2}MnO_3$, $La_{0.75}Sr_{0.25}MnO_3$ and $ZnFe_2O_4$ particles were synthesized by a freeze-drying method and their size was reduced by high-energy planetary ball milling to 100–200 nm.[114] In an AC magnetic field (800 kHz, 7.2 kA m^{-1}), the maximal temperature reached by $La_{0.75}Sr_{0.25}MnO_3$ particles was 46.3 °C (T_C = 56 °C) and 37.8 °C for $La_{0.8}Sr_{0.2}MnO_3$ particles (T_C = 48 °C) (Fig. 11). The difference between T_C and the observed maximal temperature was assigned to the sharp decrease of saturation magnetization (as is usual for ferromagnetic materials in the vicinity of T_C and predicted by ferromagnetic exchange theory) and to the heat exchange balance. No maximal temperature was found for $ZnFe_2O_4$ particles after 40 min (T_C *ca.* 100 °C), but the rise in temperature decreased as temperature increased. Lastly, yttrium aluminium iron garnet $Y_3Fe_{5-x}Al_xO_{12}$ nanoparticles were synthesized by the citrate gel process by varying the aluminium content x from 0 to 2.[115] The average diameter was *ca.* 100 nm and the Curie temperature range from −40 °C (for x = 2) to 280 °C (for x = 0). Therefore it is possible to adjust T_C at the temperature necessary for hyperthermia experiments. By interpolation, it was found that the aluminium content corresponds to value for x of about 1.5. Nevertheless, at body temperature, the magnetization of this compound (which decreases with increasing x value) is probably not high enough for heating. No experiment in an AC magnetic field was reported in this study.

Conclusion

Magnetic nanoparticles are now routinely used as contrast agents for the MPS organs (liver, spleen and bone marrow) and very soon for lymph nodes (uptake by the macrophages of the lymphatic system). It is obvious that future developments will be in the direction of active targeting through molecular imaging and cell tracking. Therefore in the case of cancer diagnosis, the next challenge for the future is the generation of functionalised surfaces of these particles.

At the same time, great efforts have led to preclinical trials of magnetic hyperthermia by using colloidal mediators. Beyond the experimental SARs, which are often 10 times lower than the expected values, the main limitation for tumour treatment is the current necessity of depositing magnetic nanoparticles

inside the tumour or through the arterial supply of the tumour. Therefore in this field, both challenges will be the design of stealth nanoparticles able to circulate in the blood compartment for a long time and the surface grafting of ligands able to facilitate their specific internalisation in tumour cells.

The strangest thing is to observe that, in the very narrow field of the *in vivo* applications of magnetic nanoparticles, the community of researchers who are involved in MR contrast agents does not overlap with the researchers who are investigating magnetic hyperthermia. A similar remark may be made after the analysis of literature cited in the papers of each community: the efforts of a community seem to be ignored by the other one. Nevertheless, day after day, it turns out that the remaining obstacles are common and the possibilities for resolving them are the same ones. Moreover, it is now accepted that superparamagnetic nanoparticles, which are efficient as MR contrast agents, exhibit the highest SAR values in clinically tolerable conditions of magnetic field amplitude and frequency. Therefore it is perhaps time for both communities to combine their efforts and dream together to a unique and versatile device which will be able to reveal tumours and metastases and subsequently treat them by hyperthermia.

In such a context, the association with drug delivery scientists would allow us to envisage wonderful breakthroughs. For instance, intracellular drug release could be triggered by the temperature increase during the hyperthermia sequence under MRI monitoring. Such a mechanism could use thermolabile bonds or thermosensitive polymers, whose macromolecules would change from a hydrophobic state to a hydrophilic one or *vice versa*, allowing the controlled entrapment and release of the drug, *e.g.* copolymers of *N*-vinylpyrrolidone and acrylic acid.[10] The day when these combined drug delivery devices will be specifically internalised in tumour cells, very efficient drugs (already known, but too toxic for systemic administration) may be used.

R. Duncan said in 1997: "The drug development process is inevitably lengthy and the breakthroughs more frequently a dream rather than reality".[11] Today, physicians, pharmacologists, biologists, chemists of organic molecules and macromolecules, physicists and chemists of solid state have to dream and to dream together, because if such a combined drug delivery device occurs one day, it will necessarily be the result of joint work.

Acknowledgements

The authors wish to thank Prof. Jacques E. Bonnet, Dr Anne-Karine Bouzier-Sore, Prof. Valérie Cabuil, Prof. Jean-Marie Caillé, Prof. Paul Canioni, Prof. Patrick Couvreur, Dr Mathilde Deloire-Grassin, Dr Marie Hélène Delville, Dr Alain Demourgues, Prof. Martine Dorian, Prof. Vincent Dousset, Dr Catherine Dubernet, Prof. Michel Fontanille, Prof. Léopold Fournès, Prof. Jean-Michel Franconi, Dr Graziella Goglio, Dr Valérie Heroguez, Dr Christine Labrugère, Ms Stéphanie Lassiaz, Mr Sylvain Miraux, Dr Klaus Petry, Dr Emil Pollert, Dr Josik Portier, Mrs Lydia Raison, Dr Fabio Sonvico, Dr Eric Thiaudière, Mr Matthieu Valle, Dr Antoine Vekris, Dr Pavel Veverka, Dr Pierre Voisin, Dr Alain Wattiaux and Dr Jeremy Boncaster for valuable collaboration and helpful discussions.

References

1 U. Häfeli, in *Magnetism in Medicine: A Handbook*, W. Andrä and H. Nowak, ed., Wiley-VCH, Berlin, 1998, p. 15.
2 R. Weissleder, G. Elizondo, J. Wittenberg, C. A. Rabito, L. Bengele and L. Josephson, *Radiology*, 1990, **175**, 489–493.
3 W. Andrä, in *Magnetism in Medicine: A Handbook*, ed. W. Andrä, and H. Nowak, Wiley-VCH, Berlin, 1998, p. 455.
4 S. M. Moghimi and J. Szebeni, *Prog. Lipid Res.*, 2003, **42**, 463–478.
5 C. Monfardini and F. M. Veroneses, *Bioconjugate Chem.*, 1998, **9**, 418–450.
6 Q. A. Pankhurst, J. Connolly, S. K. Jones and J. Dobson, *J. Phys. D: Appl. Phys.*, 2003, **36**, R167–R181.
7 M. T. Peracchia, *STP Pharma Sci.*, 2003, **13**, 155–161.
8 M. N. V. Kumar, *J. Pharm. Pharmaceut. Sci.*, 2000, **3**, 234–258.
9 S. M. Moghimi, A. C. Hunter and J. C. Murray, *Pharmacol. Rev.*, 2001, **53**, 283–318.
10 P. K. Ghosh, *Indian J. Biochem. Biophys.*, 2000, **37**, 273–282.
11 H. Pinto-Alphandary, A. Andremont and P. Couvreur, *Int. J. Antimicrob. Agents*, 2000, **13**, 155–168.
12 J. Kreuter, *Adv. Drug Delivery Rev.*, 2001, **47**, 65–81.
13 P. R. Lockman, R. J. Mumper, M. A. Khan and D. D. Allen, *Drug Dev. Ind. Pharm.*, 2002, **28**, 1–12.
14 P. Couvreur, I. Brigger and C. Dubernet, *Adv. Drug Delivery Rev.*, 2002, **54**, 631–651.
15 D. A. Hume, I. L. Ross, S. R. Himes, R. T. Sasmono, C. A. Wells and T. Ravasi, *J. Leukocyte Biol.*, 2002, **72**, 621–627.
16 S. M. Moghimi and H. M. Patel, *Adv. Drug Delivery Rev.*, 1998, **32**, 45–60.
17 S. J. Douglas, S. S. Davis and L. Illum, *CRC Crit. Rev. Ther. Drug Carrier Syst.*, 1987, **3**, 233–261.
18 N. Chiannilkulchai, Z. Driouich, J. P. Benoit, A. L. Parodi and P. Couvreur, *Sel. Cancer Ther.*, 1990, **5**, 1–11.
19 S.-W. Choi, W.-S. Kim and J.-H. Kim, *J. Dispersion Sci. Technol.*, 2003, **24**, 475–487.
20 S. M. Moghimi and A. C. Hunter, *Trends Biotechnol.*, 2000, **18**, 412–420.
21 J. T. Li, K. D. Caldxell and N. Rapoport, *Langmuir*, 1994, **10**, 4475–4482.
22 S. M. Moghimi, *Biochem. Biophys. Acta*, 1997, **1336**, 1–6.
23 S. Zalipsky, *Bioconjugate Chem.*, 1995, **6**, 150–165.
24 M. R. Kaplan, E. Calef, T. Bercovici and C. Gitler, *Biochim. Biophys. Acta*, 1983, **728**, 112–120.
25 M. Kumakura, M. Suzuki, S. Adachi and I. Kaetsu, *J. Immunol. Methods*, 1983, **63**, 115–122.
26 D. Bourel, A. Rolland, R. Le Verge and B. Genetet, *J. Immunol. Methods*, 1988, **106**, 161–167.
27 B. Stella, S. Arpicco, M. T. Peracchia, D. Desmaëlle, J. Hoebeke, M. Renoir, J. D'Angelo, L. Cattel and P. Couvreur, *J. Pharm. Sci.*, 2000, **89**, 1452–1464.
28 Y. Okuhata, *Adv. Drug Delivery Rev.*, 1999, **37**, 121–137.
29 H.-J. Weinmann, W. Ebert, B. Misselwitz and H. Schmitt-Willich, *Eur. J. Radiol.*, 2003, **46**, 33–44.
30 A. E. Merbach and E. Toth, *The Chemistry of Contrast Agents in Medical Magnetic Resonance Imaging*, John Wiley & Sons, New York, 2001.
31 R. C. Brasch, *Magn. Reson. Med.*, 1991, **22**, 282–287.
32 E. Unger, C. Tilcock, Q. F. Ahkong and T. A. Fritz, *Invest. Radiol.*, 1990, **25**, S65–S66.
33 C. H. Reynolds, N. Annan, K. Beshah, J. H. Huber, S. H. Shaber, E. Lenkinski and J. A. Worthman, *J. Am. Chem. Soc.*, 2000, **122**, 8940–8945.
34 M. E. Bernardino, S. W. Young, J. K. Lee and J. C. Weinreb, *Radiology*, 1992, **183**, 53–58.
35 A. Gustavo and Jr. Mercier, *Magn. Reson. Imaging*, 1995, **13**, 807–817.
36 B. Gallez, V. Lacour, R. Demeure, R. Debuyst, F. Dejehet, J. L. De Keyser and P. Dumont, *Magn. Reson. Imaging*, 1994, **12**, 61–69.
37 D. K. Shen, T. A. Fritz, H. F. Wu, B. Kulik, D. Palestrant and E. Unger, *Invest. Radiol.*, 1994, **29**, S217–S219.
38 S. Fallis, J. Beaty-Nosco, R. B. Dorshow and K. Adzamli, *Invest. Radiol.*, 1998, **33**, 847–852.
39 B. Bonnemain, *J. Drug Targeting*, 1998, **6**, 167–174.
40 J. W. M. Bulte, R. A. Brooks and B. M. Moskowitz, *Magn. Reson. Med.*, 1999, **42**, 379–384.
41 J. W. M. Bulte and R. A. Brooks, in *Scientific and Clinical Applications of Magnetic Carriers*, U. Häfeli, W. Schütt, J. Teller, and M. Zborowski, ed., Plenum Press, New York, 1997, p. 527.
42 P. Gillis and S. H. Koening, *Magn. Reson. Med.*, 1987, **5**, 323–345.
43 A. Roch and R. N. Muller, *Proc. Soc. Magn. Reson. Med.*, 1992, 1447.
44 R. S. Molday, *US Pat.*, 4 452 773, 1984.
45 P. Reimer and T. Balzer, *Eur. Radiol.*, 2003, **13**, 1266–1276.
46 C. Grüttner, J. Teller, W. Schütt, F. Wesphal, C. Schümichen and B.-R. Paulke, in *Scientific and Clinical Applications of Magnetic Carriers*, U. Häfeli, ed., Plenum Press, New York, 1997, p. 53.

47 C. E. Sjögren, C. Johansson, A. Naevestad, P. C. Sontum, K. Briley-Saebo and A. K. Fahlvik, *Magn. Reson. Imaging*, 1997, **15**, 55–67.
48 C. W. Jung, *Magn. Reson. Imaging*, 1995, **13**, 675–691.
49 E. V. Groman and L. Josephson, *US Pat.*, 5 248 492, 1993.
50 C. Lesniak, T. Schiestel, R. Nass and H. Schmidt, *Mater. Res. Soc. Symp. Proc.*, 1997, **432**, 169–174.
51 S. Mornet, E. Duguet and J. Portier, *French Pat.*, pending.
52 R. Weissleder, D. D. Stark, B. L. Engelstad, B. R. Bacon, C. C. Compton, D. L. White, P. Jacobs and J. Lewis, *Am. J. Roentgenol.*, 1989, **152**, 167–173.
53 M. I. Papisov, A. Bogdanov, B. Schaffer, N. Nossiff, T. Shen, R. Weissleder and T. J. Brady, *J. Magn. Magn. Mater.*, 1993, **122**, 383–386.
54 N. A. Brusentsov, V. V. Gogosov, T. N. Brusentsova, A. V. Sergeev, N. Y. Jurchenko, A. A. Kuznetsov, O. A. Kuznetsov and L. I. Shumakov, *J. Magn. Magn. Mater.*, 2001, **225**, 113–117.
55 S. Wada, L. Yue, K. Tazawa, I. Furuta, H. Nagae, S. Takemori and T. Minamimura, *Oral Diseases*, 2001, **7**, 192–195.
56 J. W. M. Bulte and M. de Cuyper, *Methods Enzymol.*, 2003, **373**, 175–198.
57 A. Bogdanov, C. Martin, R. Weissleder and T. J. Brady, *Biochim. Biophys. Acta*, 1994, **1193**, 536–542.
58 M. De Cuyper and S. Valtonen, *J. Magn. Magn. Mater.*, 2001, **225**, 89–94.
59 J. W. M. Bulte, M. de Cuyper, D. Despres and J. A. Frank, *J. Magn. Magn. Mater.*, 1999, **194**, 204–209.
60 J. W. M. Bulte, L. D. Ma, R. L. Magin, R. L. Kamman, C. E. Hulstaert, K. G. Go, T. H. The and L. de Leij, *Magn. Reson. Med.*, 1993, **29**, 32–37.
61 F. C. Meldrum, B. R. Heywood and S. Mann, *Science*, 1992, **257**, 522–523.
62 C. W. Jung and P. Jacobs, *Magn. Reson. Imaging*, 1995, **13**, 661–674.
63 J. W. M. Bulte, T. Douglas, S. Mann, R. B. Frankel, B. M. Moskowitz, R. A. Brooks, C. D. Baumgarner, J. Vymazal, M. P. Strub and J. A. Frank, *J. Magn. Reson. Imaging*, 1994, **4**, 497–505.
64 J. W. M. Bulte, T. Douglas, S. Mann, J. Vymazal, P. G. Laughlin and J. A. Frank, *Acad. Radiol.*, 1995, **2**, 871–878.
65 R. Weissleder, J. F. Heautot, B. K. Schaffer, N. Nossif, A. Papisov, A. Bogdanov and T. J. Brady, *Radiology*, 1994, **191**, 225–230.
66 R. Guimaraes, O. Clement, J. Bittoun, F. Carnot and G. Frija, *Am. J. Roentgenol.*, 1994, **162**, 201–207.
67 M.-F. Bellin, L. Lebleu and J.-B. Meric, *Abdom. Imaging*, 2003, **28**, 155–163.
68 K. E. Kellar, D. K. Fujii, W. H. H. Gunther, K. Briley-Saebo, M. Spiller and S. H. Koening, *Magn. Reson. Mater. Phys. Biol. Med.*, 1999, **8**, 207–213.
69 S. Cerdan, H. R. Lötscher, B. Künnecke and J. Seelig, *Magn. Reson. Med.*, 1989, **12**, 151–163.
70 R. Weissleder, A. S. Lee, A. J. Fischman, P. Reimer, T. Shen, R. Wilkinson, R. J. Callahan and T. J. Brady, *Radiology*, 1991, **181**, 245–249.
71 L. G. Remsen, C. I. McCormick, S. Roman-Goldstein, G. Nilaver, R. Weissleder, I. Hellstrom, R. A. Kroll and E. A. Neuwelt, *Am. J. Neuroradiol.*, 1996, **17**, 411–418.
72 Y. Zhang, N. Kohler and M. Zhang, *Biomaterials*, 2002, **23**, 1553–1561.
73 F. Sonvico, *''Mise au point de nanoparticules métalliques pour l'hyperthermie tumorale'', Thesis*, Paris-Sud University, France, 2004.
74 O. S. Nielsen, M. Horsman and J. Overgaard, *Eur. J. Cancer*, 2001, **37**, 1587–1589.
75 A. Jordan, R. Scholz, P. Wust, H. Fähling and R. Felix, *J. Magn. Magn. Mater.*, 1999, **201**, 413–419.
76 K. Overgaard and J. Overgaard, *Eur. J. Cancer*, 1972, **8**, 65–78.
77 P. Moroz, S. K. Jones and B. N. Gray, *J. Surg. Oncol.*, 2001, **77**, 259–269.
78 K. G. Hofer, *Abstracts of the 4th International Conference on Scientific and Clinical Applications of Magnetic Carriers*, 9–11 May, 2002, Tallahassee, Florida, p. 78; K. G. Hofer, *Eur. Cell. Mater.*, 2002, **3**(suppl. 2), 67–69.
79 J. B. Dubois, *Bull. Cancer/Radiother.*, 1995, **82**, 207–224.
80 S. D. Owens and P. W. Gasper, *Med. Hypotheses*, 1995, **44**, 235–242.
81 E. A. Gel'vich and V. N. Mazokhin, *Crit. Rev. Biomed. Eng.*, 2001, **29**, 77–97.
82 P. Moroz, S. K. Jones and B. N. Gray, *Int. J. Hyperthermia*, 2002, **18**, 267–284.
83 D. A. Hill, *Bioelectromagnetics*, 1985, **6**, 33–40.
84 T. Ohno, T. Wakabayashi, A. Takemura, J. Yoshida, A. Ito, M. Shinkai, H. Honda and T. Kobayashi, *J. Neuro-Oncol.*, 2002, **56**, 233–239.
85 A. Jordan, P. Wust, H. Fähling, W. John, A. Hinz and R. Felix, *Int. J. Hyperthermia*, 1993, **9**, 51–68.
86 P. C. Fannin and S. W. Charles, *J. Phys. D: Appl. Phys.*, 1991, **24**, 76–77.
87 A. Halbreich, J. Roger, J. N. Pons, D. Geldwerth, M. F. Da Silva, M. Roudier and J. C. Bacri, *Biochimie*, 1998, **80**, 379–390.
88 A. Jordan, R. Scholz, K. Maier-Hauff, M. Johannsen, P. Wust, J. Nadobny, H. Schirra, H. Schmidt, S. Deger, S. Loening, W. Lanksch and R. Felix, *J. Magn. Magn. Mater.*, 2001, **225**, 118–126.
89 R. Hergt, W. Andrä, C. G. d'Ambly, I. Hilger, W. A. Kaiser, U. Richter and H. G. Schmidt, *IEEE Trans. Magn.*, 1998, **34**, 3745–3754.
90 D. C. F. Chan, D. B. Kirpotin and P. A. Bunn, in *Scientific and Clinical Applications of Magnetic Carriers*, U. Häfeli, W. Schütt, J. Teller and M. Zborowski, ed., Plenum Press, New York, 1997, p. 607.
91 A. Jordan, T. Rheinländer, N. Waldöfner and R. Scholz, *J. Nanoparticle Res.*, 2003, **5**, 597–600.
92 M. Babincova, D. Leszczynska, P. Sourivong, P. Cicmanec and P. Babinec, *J. Magn. Magn. Mater.*, 2001, **225**, 109–112.
93 M. I. Shliomis and Y. L. Raikher, *IEEE Trans. Magn.*, 2004, **MAG-16**, 237–250.
94 P. C. Fannin, B. K. P. Scaife and S. W. Charles, *J. Magn. Magn. Mater.*, 1993, **122**, 159–163.
95 R. Hiergeist, W. Andrä, N. Buske, R. Hergt, I. Hilger, U. Richter and W. Kaiser, *J. Magn. Magn. Mater.*, 1999, **201**, 420–422.
96 R. K. Gilchrist, R. Medal, W. D. Shorey, R. C. Hanselman, J. C. Parott and C. B. Taylor, *Ann. Surg.*, 1957, **146**, 596–606.
97 P. Moroz, S. K. Jones, J. Winter and B. N. Gray, *J. Surg. Oncol.*, 2001, **78**, 22–29.
98 P. Moroz, S. K. Jones and B. N. Gray, *J. Surg. Oncol.*, 2002, **80**, 149–156.
99 P. Moroz, S. K. Jones and B. N. Gray, *J. Surg. Res.*, 2002, **105**, 209–214.
100 P. Moroz, H. Pardoe, S. K. Jones, T. G. St. Pierre, S. Song and B. N. Gray, *Phys. Med. Biol.*, 2002, **47**, 1591–1602.
101 P. Moroz, S. K. Jones, C. Metcalf and B. N. Gray, *Int. J. Hyperthermia*, 2003, **19**, 23–34.
102 R. T. Gordon, J. R. Hines and D. Gordon, *Med. Hypotheses*, 1979, **5**, 83–102.
103 A. Jordan, R. Scholz, P. Wust, H. Fähling, J. Krause, W. Wlodarczyk, B. Sander, T. Vogl and R. Felix, *Int. J. Hyperthermia*, 1997, **13**, 587–605.
104 D. C. F. Chan, D. B. Kirpotin and P. A. Dunn, *J. Magn. Magn. Mater.*, 1993, **122**, 374–378.
105 A. Jordan, P. Wust, R. Scholz, B. Tesche, H. Fahling, T. Mitrovics, T. Vogl, J. Cervos-Navarro and R. Felix, *Int. J. Hyperthermia*, 1996, **12**, 705–722.
106 A. Jordan, R. Scholz, P. Wust, H. Schirra, T. Schiestel, H. Schmidt and R. Felix, *J. Magn. Magn. Mater.*, 1999, **194**, 185–196.
107 L. Dupin, *Biofutur.*, 2003, **239**, 8.
108 M. Suzuki, M. Shinkai, M. Kamihira and T. Kobayashi, *Biotechnol. Appl. Biochem.*, 1995, **21**, 335–345.
109 M. Shinkai, M. Suzuki, S. Iijima and T. Kobayashi, *Biotechnol. Appl. Biochem.*, 1995, **21**, 125–137.
110 B. Le, M. Shinkai, T. Kitade, H. Honda, J. Yoshida, T. Wakabayashi and T. Kobayashi, *J. Chem. Eng. Jpn.*, 2001, **34**, 66–72.
111 M. Shinkai, B. Le, H. Honda, K. Yoshikawa, K. Shimizu, S. Saga, T. Wakabayashi, J. Yoshida and T. Kobayashi, *Jpn. J. Cancer Res.*, 2001, **92**, 1138–1145.
112 Y. Rabin, *Int. J. Hyperthermia*, 2002, **18**, 194–202.
113 B. Quesson, F. Vimeux, R. Salomir, J. A. de Zwart and C. T. W. Moonen, *Magn. Reson. Med.*, 2002, **47**, 1065–1072.
114 A. A. Kuznetsov, O. A. Shlyakhtin, N. A. Brusentsov and O. A. Kuznetsov, in *Abstracts of the 4th International Conference on Scientific and Clinical Applications of Magnetic Carriers*, 9–11 May, 2002, Tallahassee, Florida, p. 87; A. A. Kuznetsov, O. A. Shlyakhtin, N. A. Brusentsov and O. A. Kuznetsov, *Eur. Cell. Mater.*, 2002, **3**(suppl. 2), 75–77.
115 F. Grasset, S. Mornet, A. Demourgues, J. Portier, J. Bonnet, A. Vekris and E. Duguet, *J. Magn. Magn. Mater.*, 2001, **234**, 409–418.